Theory of magneto-optical properties of excitons in GaN

M. Sobol and W. Bardyszewski
Institute of Theoretical Physics, Warsaw University, ul. Hoża 69, 00-681 Warsaw, Poland
(Received 25 July 2005; revised manuscript received 30 November 2005; published 16 February 2006)

The magnetoexciton spectrum of wurtzite-type GaN in high magnetic field parallel to the crystal c axis is studied theoretically. The magnetic field dependence of the interband absorption spectra for various polarizations of light is obtained by solving the multisubband exciton equation in the Landau orbitals representation using the Lanczos reduction technique. Our theoretical model takes into account the hexagonal symmetry of the wurtzite GaN crystal and includes the coupling between different valence subbands. It is shown that the proposed method consistently reproduces experimental data in the wide range of magnetic fields. By comparing our results with experimental data we were able to estimate the valence band Luttinger constant $\kappa \approx 0.35$.

DOI: 10.1103/PhysRevB.73.075208 PACS number(s): 78.66.Fd, 75.50.Pp

I. INTRODUCTION

Recent interest in studying optical properties of III-V nitrides is due to their potential applications in optoelectronic devices operating in the short-wavelength spectral region. Although these materials have already been used in commercial laser diodes emitting light in the blue-violet spectral region, the detailed knowledge of their electronic band structure is still far for complete.

Wurtzite GaN is a direct band gap semiconductor. The valence band at the Γ point ($\boldsymbol{k}=0$) is split by the crystal-field and spin-orbit interaction into three subbands commonly denoted A, B, C and related to the Γ_9, Γ_{7+}, Γ_{7-} symmetry levels, respectively. Although the band structure in the vicinity of the Γ point is well described using the standard $\boldsymbol{k}\cdot\boldsymbol{p}$ method,[1] the necessary band structure parameters have to be determined experimentally or obtained from the *ab initio* calculations. Optical spectroscopy in the magnetic field supplies a wealth of data from which the key band structure parameters can be inferred with great accuracy. However the interband transitions in semiconductors are usually associated with excitonic effects and therefore an accurate model which involves both electron-hole interaction and the structure of the conduction and valence bands has to be employed in order to describe such measurements.

The purpose of this study is to provide theoretical understanding of the excitonic spectra in GaN in high magnetic field including the effect of built-in strain. Magnetoreflectance measurements for various light polarizations in the magnetic field $\mathbf{B}\|\mathbf{c}$ configuration show that the Zeeman splitting of excitons A and B is negligibly small for heteroepitaxial GaN layers grown on sapphire up to the magnetic field of 23 T. A strong broadening of the lowest C exciton transition line associated with the coupling to the continuum states of excitons A and B was also observed. The experimental data were quite well parametrized by the hydrogenic model for decoupled A, B, and C excitons in a magnetic field assuming identical effective Rydberg value for all three exciton branches.[2]

To understand this result we have developed a multiband exciton model of absorption in the presence of the magnetic field parallel to the crystal c axis, taking into account the built in biaxial strain caused by the lattice mismatch with the substrate layer. Since the energy separation between valence subbands of GaN is comparable to the exciton binding energy, the intersubband coupling should play an important role in the exciton absorption, especially in the regime of high magnetic fields. Consequently, unlike in a simple, two-band semiconductor model, there are no exact solutions for the excitonic eigenstates neither in zero nor in high magnetic fields available. It turns out, however, that the electron-hole pair $\boldsymbol{k}\cdot\boldsymbol{p}$, wurtzite symmetry Hamiltonian at zero Coulomb coupling can be exactly diagonalized for arbitrary magnetic fields. These exact eigenstates form a natural basis set in which the exciton Hamiltonian can be diagonalized. Our technique is therefore complementary to the approximation assuming the dominant role of the Coulomb interaction and treating the magnetic field as as small perturbation as discussed recently in Ref. 3.

II. EXCITON HAMILTONIAN IN THE MAGNETIC FIELD

According to the linear-response theory the absorption coefficient can be written as (we employ atomic units $\hbar=e=m_0=1$ throughout this paper)[4]

$$\alpha(\omega)=\frac{4\pi}{cn_r\omega\Omega}\,\mathrm{Re}\int_0^\infty \langle[\hat{P}_\varepsilon(t),\hat{P}_\varepsilon^+(0)]_-\rangle e^{i(\omega+i0^+)t}dt, \quad (1)$$

where Ω is the system volume, n_r—the refractive index, and the angular brackets represent ensemble averaging. We will use the abbreviation $1\equiv(m_1,\boldsymbol{k}_1,s_1)$ to denote an electron state with the wave vector $\boldsymbol{k}_1$ and spin s_1 in the band m_1. In the following analysis the indices 1 will be limited only to the states in the conduction band and the indices 2 will denote the states in the valence subbands. If we define creation a_1^+ and annihilation a_2 operators for electron band states 1 and 2 respectively then the part of the momentum operator promoting electrons from the valence to the conduction band has the form $\hat{P}_\varepsilon^\dagger(t)=\Sigma_{1,2}P_{1,2}^\varepsilon a_1^+(t)a_2(t)$, where $P_{1,2}^\varepsilon=\langle 1|\hat{p}_\varepsilon|2\rangle$ is equal to the matrix element of $\hat{p}_\varepsilon$—the projection of the one-particle momentum operator onto the light polarization

vector ε. The expectation value of the commutator in Eq. (1) can be conveniently evaluated using the correlation function $\Psi_{1,2} := \Theta(t)\langle[a_2^+(t)a_1(t), \hat{P}_\varepsilon^\dagger(0)]_-\rangle$ for which we can write the exciton equation of motion as

$$i\frac{\partial}{\partial t}\Psi_{1,2}(t) = \sum_{\bar{1},\bar{2}} (H^c_{1,\bar{1}}\delta_{2,\bar{2}} - H^v_{2,\bar{2}}\delta_{1,\bar{1}})\Psi_{\bar{1},\bar{2}}(t) - \sum_{\bar{2},\bar{1}} V_{1,\bar{2},2,\bar{1}}\Psi_{\bar{1},\bar{2}}(t) + i\delta(t)P^\varepsilon_{1,2}. \quad (2)$$

Here we have assumed that the valence band is fully occupied and the conduction band states are empty so the summation is carried over empty conduction states $\bar{1}$ and occupied valence states $\bar{2}$. The kinetic energy part of the exciton Hamiltonian is represented by the operator $H^c_{1,\bar{1}}$ which describes the conduction band states, and the valence band term $H^v_{2,\bar{2}}$ which is equal to the transposed valence band Hamiltonian matrix. In our approach the single-particle Hamiltonians $H^c_{1,\bar{1}}$ and $H^v_{2,\bar{2}}$ are expressed in the representation obtained from the Luttinger-Kohn functions by the $\boldsymbol{k}\cdot\boldsymbol{p}$ perturbation theory.[5] Coulomb interaction screened by the anisotropic static dielectric matrix is described by $V_{1,\bar{2},2,\bar{1}}$ matrix elements.

III. KINETIC PART OF THE ELECTRON-HOLE HAMILTONIAN

Optical and transport phenomena in semiconductors involve the electronic structure near the band edges. According to the theory of Luttinger and Kohn,[5,6] and Bir and Pikus[7] the Hamiltonian for the electron-hole (e-h) pair in the presence of an external magnetic field is given by a 6×6 matrix operator

$$\mathcal{H}_0 = H^c(\boldsymbol{p}_e) - H^v(\boldsymbol{p}_h). \quad (3)$$

The first term which describes the electron motion in the conduction band is treated in the parabolic and spherical band approximation. Including the Zeeman splitting with $g_0=2$ and the magnetic field directed along the z-axis, it can be written as $H^c(\boldsymbol{p}_e)=\boldsymbol{p}_e^2/2m_e^* + g_0\mu_B B_z s_{c,z} + E_g$, where $s_{c,z}$ and E_g denote the z component of the conduction band spin operator and the energy gap respectively while μ_B denotes the Bohr magneton. The second term corresponds to the hole in the valence band and takes into account the dispersion of the three subbands in the vicinity of the valence band edge. The kinetic momentum of the electron is given by $\boldsymbol{p}_e=-(i/\hbar)\boldsymbol{\nabla}_e + e\boldsymbol{A}(\boldsymbol{r}_e)$ $(e>0)$ with the vector potential assumed in the form $\boldsymbol{A}=\frac{1}{2}\boldsymbol{r}\times\boldsymbol{B}$. Using the hole momentum which is defined as $\boldsymbol{p}_h=(i/\hbar)\boldsymbol{\nabla}_h + e\boldsymbol{A}(\boldsymbol{r}_h)$ the valence band contribution to the kinetic-energy in wurtzite structure reads[1,7]

$$\begin{aligned} H^v(\boldsymbol{p}_h) = {} & \Delta_1(I_z^2-1) + \Delta_2(I_z\sigma_z - 1) + \sqrt{2}\Delta_3(I_+\sigma_- + I_-\sigma_+) \\ & + (A_1 + A_3 I_z^2)p_{hz}^2 + (A_2 + A_4 I_z^2)(p_{hx}^2 + p_{hy}^2) - A_5(I_+^2 p_{h-}^2 \\ & + I_-^2 p_{h+}^2) - 2A_6 p_z([I_z, I_+]_+ p_{h-} + [I_z, I_-]_+ p_{h+}) \\ & + g_0\mu_B B_z s_{v,z} - \mu_B(3\kappa+1)B_z I_z. \end{aligned} \quad (4)$$

The terms proportional to the $B_z s_{v,z}$ and $B_z I_z$ describe the coupling of the valence electron spin $s_{v,z}$ and angular momentum I_z with the magnetic field. The 3×3 matrices $I_{x,y,z}$ represent the components of the angular momentum operator with $I=1$. Furthermore $I_\pm = (1/\sqrt{2})(I_x \pm iI_y)$, $p_{h\pm} = p_{hx} \pm ip_{hy}$, and $\sigma_\pm = \frac{1}{2}(\sigma_x \pm i\sigma_y)$, where $\sigma_{x,y,z}$ are standard Pauli matrices. The brackets $[I_z, I_\pm]_+ = \frac{1}{2}(I_z I_\pm + I_\pm I_z)$ denote symmetrized product. The band structure constants $A_{1\cdots 6}$ and $\Delta_{1,2,3}$ are extracted either from experimental data or from *ab initio* band structure calculations. The effect of biaxial strain ϵ_{xx} introduced by the lattice mismatch between the GaN layer and the substrate is incorporated into the renormalized energy gap E_g and the crystal field parameter Δ_1:

$$E_g = E_g^0 + 2\left(a_2 - D_4 - \frac{C_{13}}{C_{33}}(a_1 - D_3)\right)\epsilon_{xx}$$

$$\Delta_1 = \Delta_1^0 + 2\left(D_4 - \frac{C_{13}}{C_{33}}D_3\right)\epsilon_{xx}, \quad (5)$$

where E_g^0 and Δ_1^0 are equal to the values of those parameters in the absence of strain. The deformation potentials a_1 and a_2 describe the band gap renormalization due to the combined rigid shift of the conduction band and valence subbands while D_3 and D_4 are responsible for the change in the relative splitting of the valence band sublevels due to the biaxial strain. The relationship between the parallel and perpendicular components of the strain tensor with respect to the layer plane involves the ratio of the stiffness coefficients C_{13} and C_{33}.[8]

In order to describe the relative motion of the electron and hole we introduce the new set of center-of-mass and relative coordinates $\boldsymbol{R}=(\boldsymbol{r}_e+\boldsymbol{r}_h)/2$, $\boldsymbol{P}=\boldsymbol{p}_e+\boldsymbol{p}_h$ and $\boldsymbol{r}=x\hat{i}+y\hat{j}+z\hat{k}=\boldsymbol{r}_e - \boldsymbol{r}_h$, $\boldsymbol{p}=(\boldsymbol{p}_e-\boldsymbol{p}_h)/2$. Then using the Lamb transformation[9] and considering only the states with zero center-of-mass momentum $\boldsymbol{P}=0$, it could be easily verified that the whole transformation amounts to substitution $\boldsymbol{p}_e \to \pi_a$ and $\boldsymbol{p}_h \to \pi_b$ in the Hamiltonian (3), where $\pi_a = -(i/\hbar)\boldsymbol{\nabla}_r + e\boldsymbol{A}(\boldsymbol{r})$ and $\pi_b = -(i/\hbar)\boldsymbol{\nabla}_r - e\boldsymbol{A}(\boldsymbol{r})$ refer only to the relative position $\boldsymbol{r}$. Finally the Hamiltonian which represents the relative motion of a free e-h pair becomes simply $H^c(\pi_a) - H^v(\pi_b)$.

It is convenient to change variables into dimensionless form and rewrite the Hamiltonian in terms of the operators

$$a = \frac{i}{\sqrt{2}}\left(\frac{1}{2}\bar{\zeta} + 2\partial_\zeta\right) \text{ and } b = \frac{i}{\sqrt{2}}\left(\frac{1}{2}\zeta + 2\partial_{\bar{\zeta}}\right), \quad (6)$$

where $\zeta = (x+iy)/l$, $\bar{\zeta} = (x-iy)/l$ and $l=(\hbar/eB)^{1/2}$ denotes the magnetic length. It is easily verified that $[a,b]_- = [a,b^\dagger]_- = [a^\dagger,b]_- = 0, [a,a^\dagger]_- = [b,b^\dagger]_- = 1$ and the e-h kinetic energy becomes

$$\mathcal{H}_0 = E_g + \hbar\omega_e\left(aa^\dagger + \frac{1}{2}\right) - \Delta_1(I_z^2 - 1) - \Delta_2(I_z\sigma_z - 1)$$
$$- \sqrt{2}\Delta_3(I_+\sigma_- + I_-\sigma_+) + \left(\frac{1}{2m_e^*} - A_1 - A_3 I_z^2\right)k^2$$
$$- 2l^{-2}(A_2 + A_4 I_z^2)\left(b^\dagger b + \frac{1}{2}\right) + 2l^{-2}A_5(I_+^2 b^2 + I_-^2 (b^\dagger)^2)$$
$$- 2\sqrt{2}l^{-1}A_6 k([I_z, I_+]_+ b + [I_z, I_-]_+ b^\dagger) + g_0\mu_B B_z s_{cz}$$
$$- g_0\mu_B B_z s_{vz} + \mu_B(3\kappa + 1)B_z I_z. \quad (7)$$

We have introduced the conduction band cyclotron frequency $\omega_e = eB/m_e^*$ and defined k as the eigenvalue of the z component of the relative momentum $p_z|k\rangle = \hbar k|k\rangle$. The relative motion can be therefore described in the basis set of Landau orbitals multiplied by a plane wave in the z direction. Our basis set states $|n,s,k\rangle$ in the cylindrical coordinates (ρ,ϕ) are then defined by

$$\psi_{nsk}(\rho,\phi,z) = \frac{1}{\sqrt{n!s!}} e^{izk}(a^\dagger)^n (b^\dagger)^s \psi_{000}(\rho), \quad (8)$$

for $n,s = 0,1,2,\ldots$, and the ground-state wave function is given by

$$\psi_{000}(\rho) = \frac{1}{l\sqrt{2\pi}} \exp\left[-\frac{\rho^2}{4l^2}\right]. \quad (9)$$

Clearly the basis functions Eq. (8) are also eigenstates of the z axis component of the angular momentum $L_z = \hbar(\zeta\partial_\zeta - \bar{\zeta}\partial_{\bar{\zeta}})$ with the magnetic quantum number $m = n - s$. Direct inspection shows that the eigenstates of the free e-h pair Hamiltonian have four good quantum numbers: the Landau level number n, the z component of the momentum k, the z component of the electron spin $s_{c,z}$, and the z component of the total angular momentum $F_z = n - s + s_{c,z} - s_{v,z} - I_z$. It is then convenient to characterize the valence band Bloch states at the Γ point with their total angular momentum $\boldsymbol{J} = \boldsymbol{I} + \boldsymbol{s}_v$ with eigenstates corresponding to $J = 1/2$ or $J = 3/2$ and $J_z = I_z + s_{v,z}$ (Appendix A). The eigenfunctions of the e-h Hamiltonian Eq. (7) are then obtained as linear combinations of products of the valence band states $|J, J_z\rangle$ and the conduction band spinors $|s_{c,z} = \pm\frac{1}{2}\rangle$:

$$|\Psi\rangle = \sum_{J=1/2,3/2} \sum_{J_z=-J}^{J}{}' f_{J,J_z} |n,s,k\rangle |J,J_z\rangle |s_{c,z}\rangle. \quad (10)$$

The prime at the summation sign means that only the states with $s \geq 0$ are defined and are included in the expansion. The coefficients f_{J,J_z} are obtained by diagonalizing the Hamiltonian (7) projected onto at most six-dimensional subspaces spanned by the states corresponding to fixed values of n, k, $s_{c,z}$, and F_z, subject to the additional condition $s = n + s_{e,z} - J_z - F_z \geq 0$ as described in Appendix A. The solutions give combined e-h Landau levels as a function of the magnetic field. In our calculations we specialized only to the optically active states for which the electron-hole Hamiltonian can be easily diagonalized.

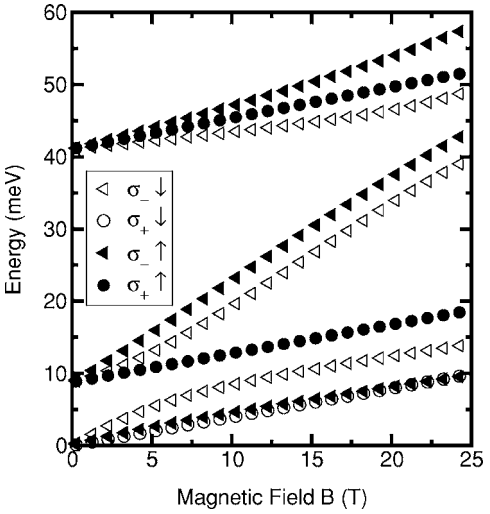

FIG. 1. Transition energies minus the energy gap for GaN as a function of the magnetic field for σ_+ (circles) and σ_- (triangles) polarizations of light for the Landau level $n = 0$. Transitions to the final states with spin down and spin up are marked with empty and filled symbols, respectively. The Coulomb interaction is neglected.

In Fig. 1 we present theoretical transition energies with $F_z = \pm 1$ corresponding to the $\sigma_\pm$ polarization of light for $n = 0$. The calculations were performed for the set of data taken from Ref. 10 and listed in Table I. The values of the deformation potentials and stiffness coefficients taken from the same reference are as follows: $a_1 = -4.9$ eV, $a_2 = -11.3$ eV, $D_3 = 8.2$ eV, $D_4 = -4.1$ eV, $C_{13} = 106$ GPa, and $C_{33} = 398$ GPa. We have assumed compressive biaxial strain $\epsilon_{xx} = \epsilon_{yy} = -0.0019$. Three families of curves correspond to the transitions associated with the A, B, and C valence subbands. The Luttinger parameter $\kappa = 0.35$ was chosen in such a way that the lowest transition energies for $\sigma_-\uparrow$ and $\sigma_+\downarrow$ are nearly degenerate. The transition energies are measured with respect to the energy gap in the strained layer.

For a fixed Landau orbital number $n = 0$ there are three allowed transition for each family. In the case of the lowest-energy transitions from the topmost valence subband A, two of them correspond to the final electron state with spin down and one with the final electron spin up. For the other two families (B and C) we have two transitions with the final state electron spin up and one with electron spin down. The interband optical transitions in the magnetic field parallel to the c axis are allowed only for the relative electron-hole angular momentum $m = n - s = 0$. Therefore the absorption selection rules are determined by the symmetry of the conduc-

TABLE I. Band parameters for GaN from Ref. 10. The values of A_i are given in the units of $\hbar^2/2m_0$.

Δ_1^0 (meV)	Δ_2 (meV)	Δ_3 (meV)	A_1	A_2	A_3	A_4	A_5	A_6	m_e
10	5.67	5.67	−7.21	−0.44	6.68	−3.46	−3.40	−4.90	0.20

tion and valence bands at the Γ point. The topmost valence subband associated with the exciton A has a twofold degenerate symmetry Γ_9 with two basis states $|11\rangle\uparrow$ and $|1-1\rangle\downarrow$, where $|II_z\rangle$ denote basis functions of the rotation group representation corresponding to the total angular momentum I. Therefore the absorption in σ_- polarization of light leads to the final electron state in the conduction band with spin up and the σ_+ polarization gives the final state with spin down. The lower valence levels B and C have both Γ_7 symmetry. The corresponding basis states are given by the linear combinations $u_B^+=ia|11\rangle\downarrow-ib|10\rangle\uparrow$, $u_B^-=a|1-1\rangle\uparrow+b|10\rangle\downarrow$ for the B level and $u_c^+=ib|11\rangle\downarrow+ia|10\rangle\uparrow$, $u_c^-=b|1-1\rangle\uparrow-a|10\rangle\downarrow$ for the C level.[3] Consequently the transitions with σ_+ and σ_- polarizations lead to the final states with spin up and down, respectively. For the Landau level $n=0$ the term proportional to the A_5 coefficient in the Hamiltonian (7) couples the valence band states $|1-1\rangle\downarrow$ with Landau subband $s=2$ and optically active state $|11\rangle$ with $s=0$ opening a new absorption channel for the A level in the light polarization σ_- and the final state spin down. Similarly, coupling between the states $|1-1\rangle\uparrow$, $s=2$ and $|11\rangle\uparrow$ with $s=0$ leads to the additional transitions in the σ_- polarization to the final state with spin up for the B and C levels.

IV. COULOMB INTERACTION

We consider the Coulomb interaction including anisotropy of the dielectric constant in the form $V(\boldsymbol{r})=e^2/\sqrt{\varepsilon_0^{\parallel}\varepsilon_0^{\perp}(x^2+y^2)+\varepsilon_0^{\perp 2}z^2}$ with $\varepsilon_0^{\perp}$ and $\varepsilon_0^{\parallel}$ denoting the dielectric constants in the direction perpendicular and parallel to the layer plane respectively. By properly rescaling the z coordinate axis we may bring this potential back to the spherical symmetric form.[3] The only effect of this rescaling is to substitute k by $k/\sqrt{\eta}$ in the Hamiltonian (7), where $\eta=\varepsilon_0^{\perp}/\varepsilon_0^{\parallel}$. With a typical value $\eta\approx 0.92$ this procedure mostly affects the electron effective mass in the z direction and slightly modifies the coupling constant A_6. Note that the parameters A_1 and A_2 which enter the coefficient in front of k^2 in this Hamiltonian almost cancel each other.

Explicit formula for the effective Coulomb interaction in the Landau level representation is derived by using the Fourier transform of the Coulomb potential

$$\left\langle n,s,k\left|\frac{1}{r}\right|n',s',k'\right\rangle=\langle n,s|V_{k-k'}(\rho)|n',s'\rangle, \tag{11}$$

where ρ denotes the projection of the three-dimensional vector $\boldsymbol{r}$ onto the xy plane and $|n,s,k\rangle$ correspond to the basis set wave function ψ_{nsk}. We have defined

$$V_{k_z}(\rho)=\int\frac{d^2q}{(2\pi)^2}\frac{4\pi}{q^2+k_z^2}e^{i\boldsymbol{q}\cdot\rho}, \tag{12}$$

where $k_z=k-k'$. Due to the rotational invariance of the Coulomb potential, the only nonvanishing matrix elements are those with $m=n-s=n'-s'=m'$. Moreover in view of the symmetry property $\langle ns|V_{k_z}|n's'\rangle=\langle sn|V_{k_z}|s'n'\rangle=\langle n's'|V_{k_z}|ns\rangle$ it is then enough to consider the case of $m\geqslant 0$ and $n\geqslant n'$. Following the derivation given in Appendix B for $p=n-n'\geqslant 0$ we obtain

$$\langle ns|V_{k_z}|n's'\rangle=(-1)^{s+s'}\sqrt{\frac{n!s'!}{n'!s!}}n'!L_{s'}^{p}(-X_0)\times U(n'+1,1-p,X_0), \tag{13}$$

where $X_0=l^2k_z^2/2$, $U(a,b,z)$ is the confluent hypergeometric function and $L_{s'}^{p}(X)$ denotes the Laguerre polynomial.[11]

Coulomb interaction mixes states $|n,s,k\rangle$ with different n and k. Therefore the excitonic eigenfunction can be represented by

$$\Psi(\mathbf{r})=\int_{-\infty}^{+\infty}dk\sum_n\sum_{J=1/2,3/2}\sum_{J_z=-J}^{J}{}'f_{J,J_z,n,k}|n,s,k\rangle|J,J_z\rangle|s_{c,z}\rangle. \tag{14}$$

In our numerical calculations we discretize the wave vector k and approximate the integral by the appropriate quadrature. This procedure has to be applied with care due to the singular character of the Coulomb potential. To this end we observe at first that the confluent hypergeometric function $U(a,b,z)$ is limited in the vicinity of $z=0$ for $b<0$ and has a logarithmic singularity at $b=1$:

$$U(a,1,z)=-\frac{1}{\Gamma(a)}[\ln z+\psi(a)+2\gamma]+O(|z\ln z|), \tag{15}$$

where $\psi(a)$ represents the digamma function and γ is the Euler's constant.[11] Consequently all diagonal elements of the Coulomb interaction for $n=n'$ have a singularity at $k_z=k-k'=0$:

$$V_{ns}(k_z)=\langle ns|V_{k_z}|ns\rangle=n!L_s^0(-X_0)U(n+1,1,X_0)=V_{ns}^S(k_z)+V_{ns}^R(k_z)\approx-[\ln X_0+\psi(n+1)+2\gamma], \tag{16}$$

where we have identified the singular part as $V_{ns}^S(k_z)=-\ln X_0$ and the regular part is $V_{ns}^R=\langle ns|V_{k_z}|ns\rangle-V_{ns}^S$. Note that

$$V_{ns}^R(k_z=0)=-[\psi(n+1)+2\gamma]. \tag{17}$$

The quadrature approximation to the integral with respect to k_z representing the multiplication of the amplitudes f by the Coulomb potential has a general form

$$\int_{k_{\min}}^{k_{\max}}dk_z'V_{ns}(k_j-k_z')f_{k_z'}\approx\sum_{i=1}^{N}w_iV_{ns}(k_j-k_i)f_{k_i}, \tag{18}$$

where $\{k_i,w_i\}_{i=1,\ldots,N}$ correspond to the nodes and weights of the quadrature. To avoid an indefinite expression which would result from $k_j=k_i$ term we split the integral as follows:

$$\int_{k_{\min}}^{k_{\max}}dk_z'V_{ns}(k_j-k_z')f_{k_z'}\approx\sum_{i\neq j}^{N}w_iV_{ns}(k_j-k_i)f_{k_i}+\Bigg[w_jV_{ns}^R(0)+\int_{k_{\min}}^{k_{\max}}dk_z'V_{ns}^S(k_j-k_z')g(k_z'-k_j)-\sum_{i\neq j}^{N}w_iV_{ns}^S(k_j-k_i)g(k_i-k_j)\Bigg]f_{k_j}. \tag{19}$$

The value of $V_{ns}^{R}(0)$ is given by Eq. (17), while $g(k)=Q_0^2/\left(\frac{1}{2}l^2k^2+Q_0^2\right)$ is a regular function of k with properly chosen cut-off parameter Q_0^2. Finally then the integral

$$\int_{k_{\min}}^{k_{\max}} dq_z' V_{ns}^{S}(k_j-k_z')g(k_z'-k_j) = -\int_{k_{\min}}^{k_{\max}} dk_z' \ln\left[\frac{1}{2}l^2(k_j-k_z')^2\right] \times \frac{Q_0^2}{\frac{1}{2}l^2(k_z'-k_j)^2+Q_0^2} \tag{20}$$

can be easily calculated analytically so that the diagonal and off diagonal matrix elements of the Coulomb potential are treated using the same quadrature.

V. ABSORPTION COEFFICIENT

Following Eq. (1) the absorption coefficient can be expressed in terms of the eigenstates $|f^{\lambda}\rangle$ of the exciton Hamiltonian and their energies ω^{λ}

$$\alpha(\omega)=\frac{4\pi^2}{cn_r\omega\Omega}\sum_{\lambda}|\langle f^{\lambda}|P^{\varepsilon}\rangle|^2\delta(\omega-\omega^{\lambda}). \tag{21}$$

Note that F_z and $s_{c,z}$ remain good quantum number for each eigenstate $|f^{\lambda}\rangle$. The overlap of the excitonic initial state $|P^{\varepsilon}\rangle$ defined by the interband matrix elements of the momentum operator and the exciton eigenstate in the representation of basis states $|nsk\rangle$ is given by $\langle f^{\lambda}|P^{\varepsilon}\rangle=\int dk\Sigma_{n,J,J_z}\bar{f}_{J,J_z,n,k}P_{J,J_z,n,k}$, where the bar over $f_{J,J_z,n,k}$ denotes complex conjugation. Using the Landau orbitals representation we obtain $P_{J,J_z,n,k}=\psi_{nsk}(0)\langle c|\boldsymbol{\epsilon p}|v\rangle$, where $\boldsymbol{\epsilon p}=(1/\sqrt{2})\times(p_x\pm ip_y)$ for a given total angular momentum $F_z=\pm 1$. Since $\psi_{nsk}(0)=\delta_{sn}/l\sqrt{2\pi}$, obviously only the states with the orbital angular momentum $m=0$ contribute to the absorption. All elements of $P_{J,J_z,n,k}$ can be expressed in terms of the single interband coupling parameter $E_p=(2/m_0)|\langle S|p_x|X\rangle|^2$ (Appendix C). To solve the excitonic eigenvalue problem we employ Lanczos reduction technique. The basis set is constructed from the initial, polarization dependent state of the exciton $|P^{\varepsilon}\rangle$. In the effective mass approximation we use the Hamiltonian matrix containing both kinetic and potential parts acting on the exciton amplitudes $f_{J,J_z,n,k}$. The Lanczos method transforms the original Hamiltonian matrix to a tridiagonal form which is then truncated to a reasonable dimension. Diagonalization of the resulting matrix provides approximate eigen spectrum as a function of the magnetic field for two circular polarizations of the light.

The expansion (14) of the excitonic states in the Landau level basis set becomes more and more inaccurate in the limit of small magnetic fields such that the magnetic length is much larger than the characteristic Bohr radius of the exciton. Therefore for all magnetic fields below critical value B_0 of the magnetic field for which Bohr radius and the magnetic length are comparable, we have employed the basis set of Landau states corresponding to this fixed field. We have applied this method to the problem of the hydrogen atom in the uniform magnetic field setting B_0 for which $\gamma=\hbar\omega_c/2E_1=(a_B/l)^2=1$, where E_1 is the hydrogen atom Bohr energy. The comparison of our results to the very accurate numerical results of Ref. 12 for the lowest four even energy levels is presented in Fig. 2. The small discrepancy between our results (dots) and the data of Ref. 12 visible for the $3s$ and $3d$ levels is caused mainly by the Lanczos approximation.

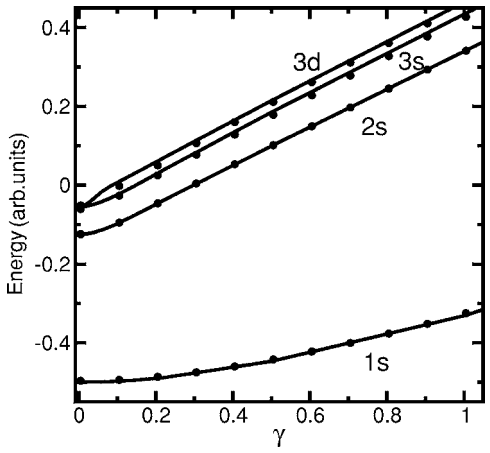

FIG. 2. The lowest four electron energy levels corresponding to even states of the hydrogen atom in the uniform magnetic field. Dots: present model, solid line: results of Ref. 12. Here $\gamma=\hbar\omega_c/2E_1$ is equal to the cyclotron frequency expressed in atomic units.

VI. RESULTS AND DISCUSSION

We have applied our theoretical method to the heteroepitaxial GaN layers grown by the MOCVD technique on sapphire.[2] The absorption spectrum for excitons A, B, C as a function of the magnetic field ($\mathbf{B}\|\mathbf{c}$) was obtained taking into account full wurtzite symmetry Hamiltonian. In our analysis we have determined both the energies and oscillator strengths for excitonic transitions in the low energy part of the absorption spectrum. All band parameters except for two were taken from the literature (see Table I). In order to obtain a reasonable fit to the experimental data we have assumed the strain free energy gap $E_g^0=3.5015$ eV and the Luttinger parameter $\kappa=0.35$. We have used the averaged static dielectric constant $\varepsilon_0=8.9$.[14] It turned out that the theoretical spectrum is not very sensitive to the dielectric function anisotropy. Applying the anisotropy factor $\eta=0.92$ we have found that the energy of the lowest transition increases by 0.6 meV at $B=25T$ and the change is even smaller for higher energies. It seems therefore that the fully spherical approximation to the screening is quite accurate. The comparison between our model with $\eta=1$ and the experimental data taken from Ref. 2 is presented in Fig. 3. The theoretical results represented by dots reproduce fairly well the positions of experimental transition energies depicted by squares. We have included 70 Landau levels to describe the electron-hole motion in the xy plane and 31 plane waves in the z direction in our calculations. For the critical magnetic field we have assumed $B_0=9T$. The transitions to the A and B excitonic ground states

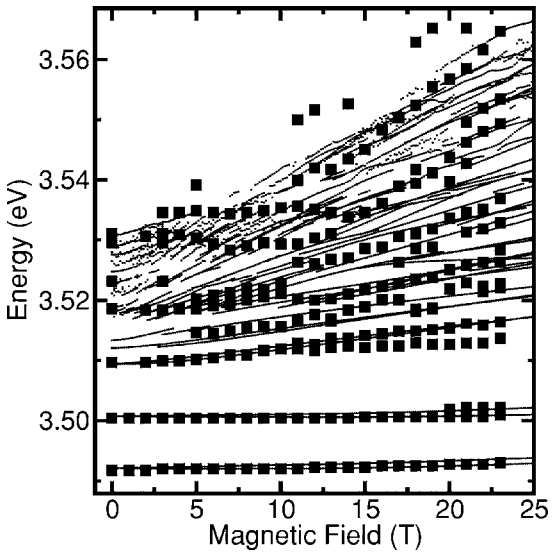

FIG. 3. Magnetic field dependence of excitonic transition energies in GaN for σ_+ and σ_- polarization. Experimental data from Ref. 2 are shown as black squares, and the calculated results are represented by dots.

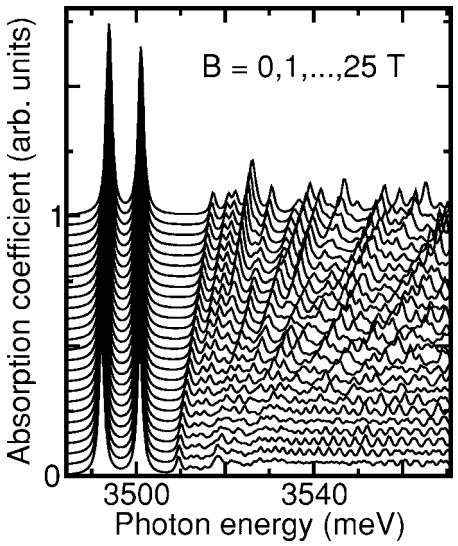

FIG. 4. Theoretical interband absorption coefficient in the polarization σ_-, in the magnetic fields $B=0-25$ T increasing from bottom to top in increments of 1 T.

and their Zeeman splittings are quite accurately described up to $B=25$ T confirming to some extend the reliability of band parameters given in Ref. 10. Due to the resonant coupling of the C exciton to the scattering states of the lower excitons A and B, the theoretical predictions for this exciton can be only observed as a series of a great number of avoided crossings of theoretical lines for energies in the vicinity of 3.53 eV. Proper visualization of this resonant transition requires plotting the spectral density for absorption including the broadening of the resonant lines which is not experimentally available. An example of theoretical absorption curves for various magnetic field values is given in Fig. 4. We have assumed the lorentzian line shape for each half absorption line with constant half width at half maximum equal to 0.7 meV.

Having determined the absorption curves and using the Kramers-Krönig transformation we may also calculate the frequency dependent refractive index and therefore the reflection coefficient. However, this calculation is very sensitive to the accuracy of the line shape model for each transition.

In conclusion we have presented a theoretical model of the near-band-edge magneto-optical absorption spectrum of three almost totally decoupled excitons A, B, C associated with split valence bands Γ_9, Γ_7, and Γ_7 symmetries. To obtain the absorption spectra we have formulated exciton equations in the framework of the $\boldsymbol{k}\cdot\boldsymbol{p}$ approximation. We have first evaluated the kinetic and potential part of the Hamiltonian in the Landau orbitals basis set. It turned out that the exact values of the free electron-hole transition energies in the magnetic fields can be obtained by diagonalizing simple 6×6 effective Hamiltonian matrices. For obtaining the magnetoexciton absorption spectra we have employed Lanczos reduction for solving a large eigen-value problem. By comparing theoretical and experimental results for a given sample we were able to estimate the Luttinger coupling parameter κ. Our method successfully reproduces not only the excitonic ground state but also the excited state transitions. In particular we are able to model the behavior of the resonant transitions related to the exciton C.

ACKNOWLEDGMENTS

We thank R. Stępniewski and A. Wysmołek for stimulating discussions of the work.

APPENDIX A: MATRIX REPRESENTATION OF THE KINETIC ENERGY HAMILTONIAN

The valence band states $|J,J_z\rangle$ are constructed from the Bloch states $|I,I_z\rangle$ at the Γ point transforming according to the rotation group representation $I=1$ and valence band spinors $|s_{v,z}\rangle=|\pm\frac{1}{2}\rangle$:

$$\begin{bmatrix} \left|\frac{3}{2},\pm\frac{3}{2}\right\rangle \\ \left|\frac{3}{2},\pm\frac{1}{2}\right\rangle \\ \left|\frac{1}{2},\pm\frac{1}{2}\right\rangle \end{bmatrix} = \begin{bmatrix} 1 & 0 & 0 \\ 0 & \frac{1}{\sqrt{3}} & \sqrt{\frac{2}{3}} \\ 0 & \pm\sqrt{\frac{2}{3}} & \mp\frac{1}{\sqrt{3}} \end{bmatrix} \begin{bmatrix} |1,\pm 1\rangle\left|\pm\frac{1}{2}\right\rangle \\ |1,\pm 1\rangle\left|\mp\frac{1}{2}\right\rangle \\ |1,\pm 0\rangle\left|\pm\frac{1}{2}\right\rangle \end{bmatrix}. \tag{A1}$$

The kinetic energy matrix elements in the representation $\{|\frac{3}{2},\frac{3}{2}\rangle,|\frac{3}{2},-\frac{3}{2}\rangle,|\frac{3}{2},-\frac{1}{2}\rangle,|\frac{3}{2},\frac{1}{2}\rangle,|\frac{1}{2},-\frac{1}{2}\rangle,|\frac{1}{2},\frac{1}{2}\rangle\}$ for given n, $s_{c,z}$, k, and F_z are most conveniently expressed by defining $s_0=n+s_{c,z}-F_z$. According to the condition $s_0-J_z=s\geqslant 0$, only states with $J_z\leqslant s_0$ exist in the expansion (10) and (14). Below we give general expressions for the kinetic energy matrix elements for $s_0\geqslant\frac{3}{2}$. The matrices for $s_0<\frac{3}{2}$ are obtained by removing the rows and columns corresponding to $J_z>s_0$:

$$\mathcal{H}_0 = \begin{bmatrix} \mathcal{P}_1 + \mathcal{E}_c & 0 & \mathcal{M}s_1 s_2 & -\mathcal{N}s_1 & -\sqrt{2}\mathcal{M}s_1 s_2 & \frac{2}{\sqrt{2}}\mathcal{N}s_1 \\ & \mathcal{P}_2 + \mathcal{E}_c & \mathcal{N}s_3 & \mathcal{M}s_2 s_3 & \frac{2}{\sqrt{2}}\mathcal{N}s_3 & \sqrt{2}\mathcal{M}s_2 s_3 \\ & & \mathcal{R}_1 + \mathcal{E}_c & 0 & \mathcal{Q}_1 & -\sqrt{\frac{3}{2}}\mathcal{N}s_2 \\ & h.c & & \mathcal{R}_2 + \mathcal{E}_c & -\sqrt{\frac{3}{2}}\mathcal{N}s_2 & \mathcal{Q}_2 \\ & & & & \mathcal{T}_1 + \mathcal{E}_c & 0 \\ & & & & & \mathcal{T}_2 + \mathcal{E}_c \end{bmatrix},$$

$$\mathcal{E}_c = E_g + \hbar\omega_e\left(n + \frac{1}{2}\right) + \frac{\hbar^2 k^2}{2m_e^*} + \mu_B B_z g_0 s_{c,z}, \qquad \mathcal{M} = \frac{2\sqrt{3}}{3}A_5 l^{-2}, \quad \mathcal{N} = \frac{2\sqrt{3}}{3}A_6 l^{-1}k,$$

$$\mathcal{P}_1 = -(A_1 + A_3)k^2 - 2(A_2 + A_4)l^{-2}(s_0 - 1) + \mu_B B_z(g_0/2 - 1 - 3\kappa),$$

$$\mathcal{P}_2 = -(A_1 + A_3)k^2 - 2(A_2 + A_4)l^{-2}(s_0 + 1) - \mu_B B_z(g_0/2 - 1 - 3\kappa),$$

$$\mathcal{R}_1 = \frac{2}{3}(\Delta_1 + 2\Delta_2 - 2\Delta_3) - \left(A_1 + \frac{1}{3}A_3\right)k^2 - 2\left(A_2 + \frac{1}{3}A_4\right)l^{-2}(s_0 + 1) - \frac{1}{3}\mu_B B_z(g_0/2 - 1 - 3\kappa),$$

$$\mathcal{R}_2 = \frac{2}{3}(\Delta_1 + 2\Delta_2 - 2\Delta_3) - \left(A_1 + \frac{1}{3}A_3\right)k^2 - 2\left(A_2 + \frac{1}{3}A_4\right)l^{-2}s_0 + \frac{1}{3}\mu_B B_z(g_0/2 - 1 - 3\kappa),$$

$$\mathcal{T}_1 = \frac{1}{3}(\Delta_1 + 5\Delta_2 + 4\Delta_3) - \left(A_1 + \frac{2}{3}A_3\right)k^2 - 2\left(A_2 + \frac{2}{3}A_4\right)l^{-2}(s_0 + 1) + \frac{2}{3}\mu_B B_z(g_0/4 + 1 + 3\kappa),$$

$$\mathcal{T}_2 = \frac{1}{3}(\Delta_1 + 5\Delta_2 + 4\Delta_3) - \left(A_1 + \frac{2}{3}A_3\right)k^2 - 2\left(A_2 + \frac{2}{3}A_4\right)l^{-2}s_0 - \frac{2}{3}\mu_B B_z(g_0/4 + 1 + 3\kappa),$$

$$\mathcal{Q}_1 = \frac{\sqrt{2}}{3}(\Delta_1 - \Delta_2 + \Delta_3 + A_3 k^2) + \frac{2\sqrt{2}}{3}A_4 l^{-2}(s_0 + 1) - \frac{\sqrt{2}}{3}\mu_B B_z(g_0 + 1 + 3\kappa),$$

$$\mathcal{Q}_2 = -\frac{\sqrt{2}}{3}(\Delta_1 - \Delta_2 + \Delta_3 + A_3 k^2) - \frac{2\sqrt{2}}{3}A_4 l^{-2}s_0 - \frac{\sqrt{2}}{3}\mu_B B_z(g_0 + 1 + 3\kappa),$$

$$s_1 = \sqrt{s_0 - \frac{1}{2}}, \quad s_2 = \sqrt{s_0 + \frac{1}{2}}, \quad s_3 = \sqrt{s_0 + \frac{3}{2}}. \tag{A2}$$

APPENDIX B: COULOMB MATRIX ELEMENTS

Below we outline the derivation of the Coulomb matrix elements in the Landau levels basis set. We employ the identity

$$\langle n_1 s_1|e^{i\mathbf{k}\cdot\rho}|n_2 s_2\rangle = (-1)^{s_1+s_2} i^{(n_1-s_1-n_2+s_2)} e^{-i\Phi(n_1-s_1-n_2+s_2)} I_{n_1 n_2} \times\left(\frac{1}{2}|K|^2\right) I_{s_1 s_2}\left(\frac{1}{2}|K|^2\right), \tag{B1}$$

where $K=(k_x+ik_y)l$ and $\Phi=\arg(K)$. The function $I_{ns}(x)$ is given by [Ref. 13, Eq. (A1.5)]:

$$I_{ns}(X) = \frac{1}{\sqrt{n!s!}} X^{(s-n)/2} e^{X/2} \frac{d^s}{dX^s}(X^n e^{-X}) = (-1)^{n-s} I_{sn}(X). \tag{B2}$$

Then simple change of the integration variable and using the definition (B2) yields

$$\langle ns|V_{k_z}|n's'\rangle = (-1)^{s+s'} \sqrt{\frac{s'!}{n'!n!s!}} \times \int_0^\infty \frac{dX}{X+X_0} L^p_{s'}(X) \frac{d^{n'}}{dX^{n'}}(X^n e^{-X}), \tag{B3}$$

where $L^p_{s'}(X)$ denotes the Laguerre polynomial

$$L^p_{s'}(X) = \frac{1}{n!} e^X X^{-p} \frac{d^{s'}}{dX^{s'}}(X^{s'+p} e^{-X}), \tag{B4}$$

and $p=s-s'=n-n'\geqslant 0$, $X_0=l^2k_z^2/2$. Integrating by parts n' times leads to

$$\langle ns|V_{k_z}|n's'\rangle = (-1)^{s+s'} \sqrt{\frac{s'!}{n'!n!s!}} n'! L^p_{s'}(-X_0) X_0^{(n-n')} \times \int_0^\infty \frac{X^n e^{-XX_0} dX}{(1+X/X_0)^{n'+1}}. \tag{B5}$$

The latter integral is related to the hypergeometric confluent function $\Gamma(a)U(a,b,z)=\int_0^\infty e^{-zt}t^{a-1}(1+t)^{b-a-1}dt$ so that

$$\langle ns|V_{k_z}|n's'\rangle = (-1)^{s+s'} \sqrt{\frac{n!s'!}{n'!s!}} n'! L^p_{s'}(-X_0) X_0^{(n-n')} \times U(n+1,p+1,X_0). \tag{B6}$$

Using the property $U(a,1-N,z)=z^N U(a+N,1+N,z)$ we arrive at the final expression (13).

APPENDIX C: SELECTIONS RULES

The selection rules follow from the fact that the only nonvanishing elements of the initial vector $|P_e\rangle$ correspond to $m=0$. It can be shown that in the basis set given by Eq. (A1) for the electron spin $\sigma_c=\pm\frac{1}{2}$ and $F_z=1$ the nonvanishing elements are, respectively,

$$\left\langle \frac{1}{2}\middle| \frac{1}{\sqrt{2}}(\hat{p}_x+i\hat{p}_y)\middle| \frac{3}{2}-\frac{1}{2}\right\rangle = \frac{1}{\sqrt{3}}\langle S|\hat{p}_x|X\rangle,$$

$$\left\langle \frac{1}{2}\middle| \frac{1}{\sqrt{2}}(\hat{p}_x+i\hat{p}_y)\middle| \frac{1}{2}-\frac{1}{2}\right\rangle = -\frac{2}{\sqrt{6}}\langle S|\hat{p}_x|X\rangle,$$

$$\left\langle -\frac{1}{2}\middle| \frac{1}{\sqrt{2}}(\hat{p}_x+i\hat{p}_y)\middle| \frac{3}{2}-\frac{3}{2}\right\rangle = \langle S|\hat{p}_x|X\rangle$$

and for $F_z=-1$.

$$\left\langle \frac{1}{2}\middle| \frac{1}{\sqrt{2}}(\hat{p}_x-i\hat{p}_y)\middle| \frac{3}{2}\frac{3}{2}\right\rangle = -\langle S|\hat{p}_x|X\rangle,$$

$$\left\langle -\frac{1}{2}\middle| \frac{1}{\sqrt{2}}(\hat{p}_x-i\hat{p}_y)\middle| \frac{3}{2}\frac{1}{2}\right\rangle = -\frac{1}{\sqrt{3}}\langle S|\hat{p}_x|X\rangle,$$

$$\left\langle -\frac{1}{2}\middle| \frac{1}{\sqrt{2}}(\hat{p}_x-i\hat{p}_y)\middle| \frac{1}{2}\frac{1}{2}\right\rangle = -\frac{2}{\sqrt{6}}\langle S|\hat{p}_x|X\rangle.$$

[1] S. L. Chuang and C. S. Chang, Phys. Rev. B **54**, 2491 (1996).

[2] A. Wysmołek, M. Potemski, R. Stępniewski, K. Pakuła, J. M. Baranowski, G. Martinez, and P. Wyder, in *Proceedings of the International Workshop on Nitride Semiconductors 2000* [IPAP Conf. Ser.**1**, 583 (2000)].

[3] A. V. Rodina, M. Dietrich, A. Göldner, L. Eckey, A. Hoffmann, Al. L. Efros, M. Rosen, and B. K. Meyer, Phys. Rev. B **64**, 115204 (2001).

[4] W. Bardyszewski, D. Yevick, Y. Liu, C. Rolland, and S. Bradshaw, J. Appl. Phys. **80**, 1136 (1996).

[5] J. M. Luttinger and W. Kohn, Phys. Rev. **97**, 869 (1955).

[6] J. M. Luttinger, Phys. Rev. **102**, 1030 (1956).

[7] G. L. Bir and G. E. Pikus, *Symmetry and Strain-Induced Effects in Semiconductors* (Wiley, New York, 1974).

[8] W. Shan, R. J. Hauenstein, A. J. Fischer, J. J. Song, W. G. Perry, M. D. Bremser, R. F. Davis, and B. Goldenberg, Phys. Rev. B **54**, 13460 (1996).

[9] W. E. Lamb Jr., Phys. Rev. **85**, 259 (1952).

[10] I. Vurgaftman and J. R. Meyer, J. Appl. Phys. **94**, 3675 (2003).

[11] *Handbook of Mathematical Functions with Formulas, Graphs and Mathematical Tables*, edited by M. Abramowitz and I. A. Stegun (National Bureau of Standards, Washington, D.C., 1972).

[12] P. C. Makado and N. C. McGill, J. Phys. C **19**, 873 (1986).

[13] P. Pröschel, W. Rösner, G. Wunner, H. Ruder, and H. Herold, J. Phys. B **15**, 1959 (1982).

[14] S. N. Mohammad and H. Morkoç, Prog. Quantum Electron. **20**, 361 (1996).